Assessing forest metrics with a ground-based scanning lidar

Chris Hopkinson, Laura Chasmer, Colin Young-Pow, and Paul Treitz

Abstract: A ground-based scanning lidar (light detection and ranging) system was evaluated to assess its potential utility for tree-level forest mensuration data extraction. Ground-based-lidar and field-mensuration data were collected for two forest plots: one located within a red pine (*Pinus resinosa* Ait.) plantation and another in a mixed deciduous stand dominated by sugar maple (*Acer saccharum* Marsh.). Five lidar point cloud scans were collected from different vantage points for each plot over a 6-h period on 5 July 2002 using an Optech Inc. ILRIS-3D laser imager. Field-validation data were collected manually over several days during the same time period. Parameters that were measured in the field or derived from manual field measures included (*i*) stem location, (*ii*) tree height, (*iii*) stem diameter at breast height (DBH), (*iv*) stem density, and (*v*) timber volume. These measures were then compared with those derived from the ILRIS-3D data (i.e., the lidar point cloud data). It was found that all parameters could be measured or derived from the data collected by the ground-based lidar system. There was a slight systematic underestimation of mean tree height resulting from canopy shadow effects and suboptimal scan sampling distribution. Timber volume estimates for both plots were within 7% of manually derived estimates. Tree height and DBH parameters have the potential for objective measurement or derivation with little manual intervention. However, locating and counting trees within the lidar point cloud, particularly in the multitiered deciduous plot, required the assistance of field-validation data and some subjective interpretation. Overall, ground-based lidar demonstrates promise for objective and consistent forest metric assessment, but work is needed to refine and develop automatic feature identification and data extraction techniques.

Résumé : Un radar optique lidar (détection et télémétrie par la lumière) basé au sol a été évalué pour son utilité potentielle dans l'estimation des données dendrométriques d'arbres individuels en forêt. Les données du lidar basé au sol et les données dendrométriques prises sur le terrain ont été collectées dans deux places-échantillons : l'une dans une plantation de pin rouge (*Pinus resinosa* Ait.) et l'autre dans un peuplement feuillu mélangé dominé par l'érable à sucre (*Acer saccharum* Marsh.). Cinq balayages constitués d'un nuage de points lidar ont été effectués dans chaque place-échantillon à partir de différents points d'observation. Ces balayages ont été réalisés sur une période de 6 h, le 5 juillet 2002, en utilisant un système d'imagerie au laser ILRIS-3D de la compagnie Optech Inc. Les données de terrain nécessaires à la validation ont été collectées manuellement sur plusieurs jours durant la même période. Les attributs mesurés sur terrain ou dérivés à partir de ces mesures comprennent : (*i*) la localisation des tiges, (*ii*) la hauteur des arbres, (*iii*) le diamètre à hauteur de poitrine (DHP), (*iv*) la densité des tiges et (*v*) le volume de bois. Ces mesures ont ensuite été comparées à celles qui ont été dérivées des données obtenues avec le système ILRIS-3D (i.e., les données du nuage de points lidar). Tous les attributs ont pu être mesurés ou dérivés à partir des données du radar optique lidar basé au sol. La hauteur moyenne des arbres a été légèrement sous-estimée à cause de l'effet d'ombrage du couvert et de la distribution sous-optimale de l'échantillonnage par balayage. Les estimations du volume de bois des deux places-échantillons sont en deçà de 7 % des estimations obtenues avec les données récoltées manuellement sur le terrain. La hauteur et le DHP des arbres peuvent être objectivement mesurés ou dérivés avec peu d'intervention manuelle. Cependant, la localisation et le dénombrement des tiges à partir du balayage constitué d'un nuage de points lidar nécessitent le recours à des données de validation sur le terrain et quelques interprétations subjectives, particulièrement pour les places-échantillons dans les peuplements feuillus à étages multiples. Dans l'ensemble, le radar optique lidar basé au sol est prometteur pour l'estimation objective et consistante des attributs forestiers, mais des efforts sont nécessaires pour raffiner et développer des techniques automatiques d'identification de certaines caractéristiques et d'extraction des données.

[Traduit par la Rédaction]

Received 4 April 2003. Accepted 17 September 2003. Published on the NRC Research Press Web site at http://cjfr.nrc.ca on 12 March 2004.

C. Hopkinson[1] and L. Chasmer. Laboratory for Remote Sensing of Earth and Environmental Systems, Department of Geography, Mackintosh–Corry Hall, Queen's University, Kingston, ON K7L 3N6, Canada, and Otterburn Geographic, 387 Nelson Street, Kingston, ON K7K 4M9, Canada.
C. Young-Pow. Optech Incorporated, 100 Wildcat Road, North York, ON M3J 2Z9, Canada.
P. Treitz. Laboratory for Remote Sensing of Earth and Environmental Systems, Department of Geography, Mackintosh–Corry Hall, Queen's University, Kingston, ON K7L 3N6, Canada.

[1]Corresponding author (e-mail: chopkinson@cogeco.ca).

 doi: 10.1139/X03-225

Introduction

Plot-level tree volume is traditionally estimated using species- and site-dependent allometric relationships with tree height, diameter at breast height (DBH), and stem density (Schumacher and Hall 1933). Manually collecting these forest inventory parameters in the field can be time consuming, costly, and susceptible to subjective errors. This is often the case with tree height estimates using standard optical methods, where accuracy is limited by the interaction of the observer, instrument, and stand conditions (Bruce 1975). In addition, adverse site conditions (e.g., dense vegetation or swamp) can make access and inventory measurements difficult to obtain. With recent advances in ground-based laser survey technologies (Lichti et al. 2000, 2002), the potential for automated, noninvasive, objective, and expedient field mensuration of these important plot-level tree attributes is now becoming a possibility.

Laser-ranging survey technology, or lidar (light detection and ranging), takes advantage of the constancy of the speed of light by transmitting laser pulses from a known source to a target and timing the period between pulse transmission and reception of the reflected pulse (Bachman 1979). The distance from the source (the laser head) to the target (the point of pulse reflection) is half of the product of the speed of light and the total time from pulse transmission to reception. The range and intensity (return signal strength) associated with each pulse (discrete or full waveform) is typically computed by an onboard processing unit and stored within a data storage module. Scanning mirrors can be employed to redirect laser pulses to either side of the laser head nadir axis, thus facilitating range measurements across a wide field of view. To register the lidar range data to a known coordinate reference frame, either the location and orientation of the laser head at the time of pulse transmission must be known or control points must be collected within the lidar field of view for subsequent data registration. Commercially available lidar survey instruments currently take the form of simple laser rangefinders (often employed in the electronic distance measurement units of total stations), mobile (usually airborne) laser scanners (Baltsavias 1999), or dual-axis scanning three-dimensional laser imagers (Lichti et al. 2002).

Since the early to mid 1980s, the use of lidar for forest mensuration has advanced with the technology. For example, research using early generation airborne full waveform lidar sensors has been directed towards forest inventory surveys (Aldred and Bonner 1985), merchantable timber volume estimation (Maclean and Martin 1984), and forest canopy characterization (Nelson et al. 1984). More recently, several researchers have applied new generation commercially available discrete pulse airborne lidar sensors to the task of stand-level tree height estimation (e.g., Naesset 1997*a*; Magnussen and Boudewyn 1998) and height-based timber volume estimates (e.g., Naesset 1997*b*; Lim et al. 2003*a*). In general, it is found that airborne lidar estimates of tree height tend to slightly underestimate ground-truth measurements. For a summary of research into airborne lidar technology for forest mensuration purposes, the reader is referred to Lim et al. (2003*b*).

Some studies have used ground-based lidar and laser imaging technology for forest structural assessments (summarized below), but all of these have required manually intensive data collection procedures and have been conducted over small sample plots. Most of the research to date has concentrated on the use of simple lidar instruments (rangefinders) for mapping two-dimensional canopy cross sections and gap fractions (Welles and Cohen 1996), and vertical leaf area index profiles (Radtke and Bolstad 2001). Visible laser scanners have been combined with optical cameras to measure tree structure both in the laboratory (Manninen et al. 1999) and in the field (Tanaka et al. 1998). In the study by Tanaka et al. (1998), the laser imaging system was tested in three different configurations to assess (*i*) tree positions and stem diameter, (*ii*) vertical canopy structure, and (*iii*) canopy surface shape. The study demonstrated that at distances up to and just over 10 m from the imaging system, accurate estimates of stem diameter could be obtained (Tanaka et al. 1998). Recent work carried out by Lovell et al. (2003) has shown that ground-based scanning lidar instruments can be used for foliage angle and distribution mapping and leaf area index estimation to within 8% of hemispherical photograph techniques.

The potential of this technology for forest mensuration applications is clear but as yet not fully realized. This paper presents an evaluation of a ground-based scanning lidar system for semiautomatic tree height and DBH measurements for the purpose of plot-level volume estimation within a conifer plantation and a mixed deciduous stand. Coregistration of manually surveyed and lidar-derived tree locations is also assessed as a first step towards plot-level lidar tree stem mapping.

Study area

For this study, two distinctly different site types common within the southern Ontario geographical context were selected for study: (*i*) a mature red pine (*Pinus resinosa* Ait.) plantation with no understory, and (*ii*) a multitiered mixed deciduous stand, dominated by sugar maple (*Acer saccharum* Marsh.).

Both of these sites are located in the north tract of the York Regional Forest (generally referred to as "Vivian Forest") approximately 50 km north of Toronto (Fig. 1). Lidar forest research has been ongoing within this area since the summer of 2000 (e.g., Hopkinson et al. 2004). In subsequent discussion, the two plots are referred to as plot C (red pine plantation) and plot D (deciduous stand). Each plot measured 35 m × 35 m.

Methods

Field data collection

All field data were collected from 4–17 July 2002. All trees in both plots were uniquely numbered with aluminum tags prior to measuring each tree's position, height, and DBH to enable comparison with equivalent lidar-derived forest metric information.

Stem map

The method adopted for locating 73% of the trees within plot C and a central reference tree in plot D was to use an inertial survey instrument known as the POS LS (position orientation system – land survey), manufactured and oper-

Fig. 1. Vivian Forest ILRIS-3D sample plots, 50 km north of Toronto. Plot C is a mature red pine plantation; plot D is a multitiered mixed deciduous stand (mainly sugar maple). Air photograph acquired in fall 1999.

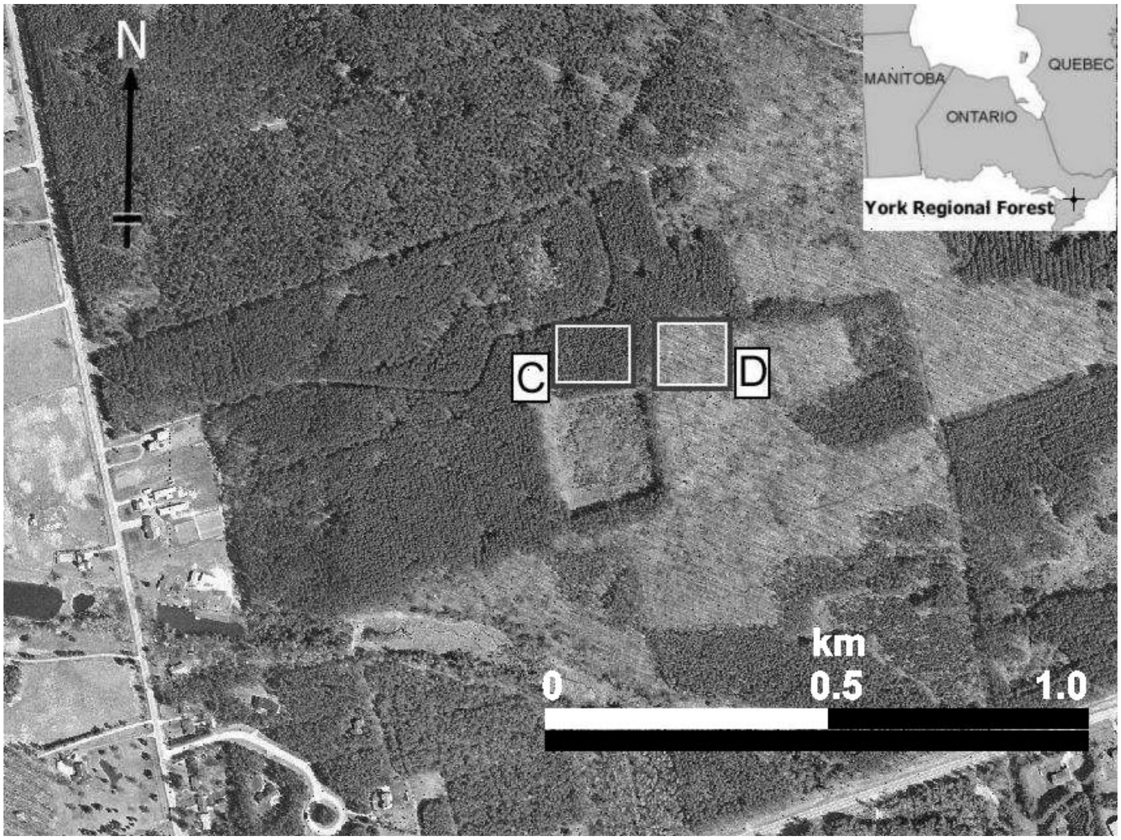

ated by Applanix Inc. (Toronto, Ont.). This system uses an inertial measurement unit and differential global positioning system (DGPS), similar to those used for airborne survey and missile guidance, to enable highly accurate four-dimensional positioning. The inertial measurement unit precisely monitors three-dimensional accelerations through time to keep a constant fix on current position. Therefore, with a known initialization point and occasional communication with a global positioning system satellite, the POS LS system can be placed next to tree stems to accurately survey tree locations even beneath a dense forest canopy. For the POS LS survey, data were referenced to a benchmark approximately 1 km west of the plots.

After completing the POS LS survey, the instrument was taken back to the initialization point so that the total amount of instrument drift could be measured and corrected for. These data possess a high level of planimetric accuracy with a 1 σ real-time measurement error of <1 m per kilometre traveled, and combined postprocessed DGPS measurements approaching a 1 σ error value of 0.05 m (Applanix Inc. 2001). It was not possible to survey all the trees in this manner because of the limited availability of the POS LS instrument and crew. The remaining trees were located using distance and bearings to triangulate tree positions from known locations. For plot C, the triangulation procedure did not introduce large errors in the tree locations, since trees of unknown location were always in close proximity to trees of known location. However, for plot D all trees were triangulated to the central "control" tree stem surveyed by the POS LS, and planimetric errors associated with measuring tape and compass bearing precision could exceed 2 m in X and Y at the edges of the plot.

Tree height

Tree heights were measured from the ground to the top of the live crown using a Vertex sonic clinometer (Haglof, Madison, Miss.). Clinometer height measurements in the deciduous plot were challenging at times, as it was difficult to observe the ground and treetops through the multitiered canopy and dense leafy biomass. This was generally not a problem in the uniform conifer plantation. Those trees for which a clear line of sight to either ground or treetop level was not possible were measured three times from different locations, and the three measurements were averaged.

Stem DBH

Tree stem DBH (1.3 m above ground) was measured for all trees using a DBH tape measure. For this study, DBH was measured for all trees with a height of 2 m or greater to enable a wide range of measurements for comparison with lidar-derived estimates.

Lidar data collection

The ground-based scanning lidar sensor used for this study was an eye-safe tripod-mounted ILRIS-3D sensor (Optech Inc., North York, Ont.), which emits 2000 laser pulses per second across a horizontal and vertical field of view of 40°. Either the first or last pulse reflected back to the unit from each pulse emitted can be directly digitized and stored, and ranges of up to 1 km can be recorded. The

Fig. 2. ILRIS-3D base station locations around the conifer plot C (left) and deciduous plot D (right). (Universal Transverse Mercator easting and northing coordinates have been truncated.)

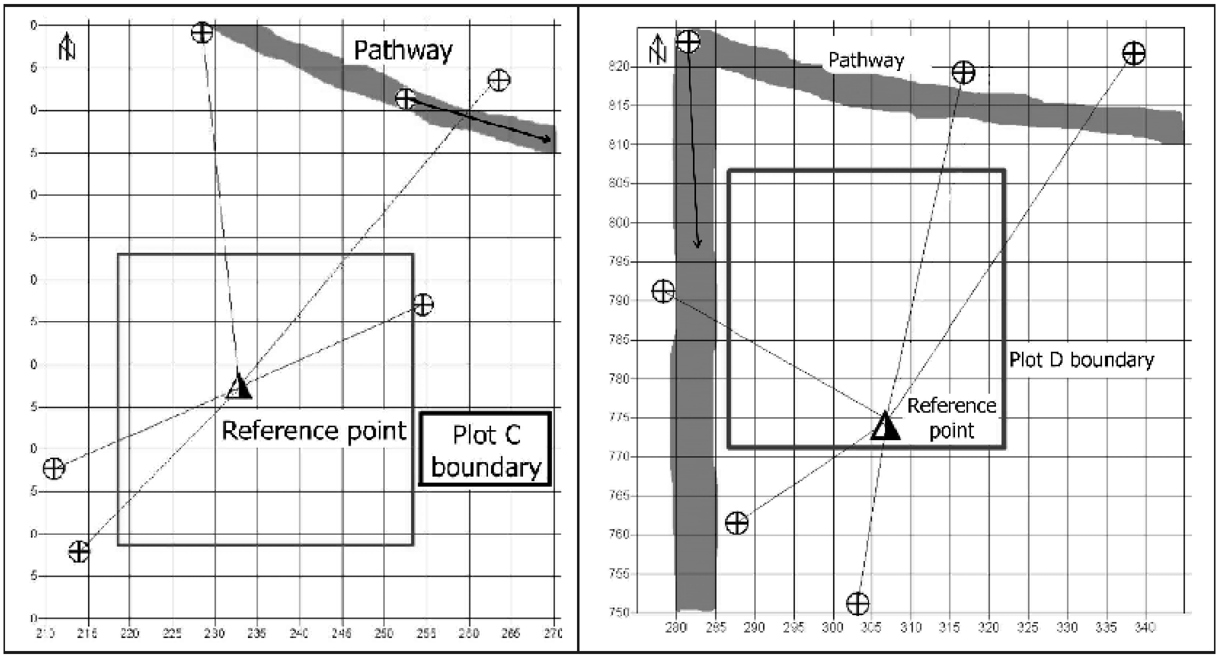

scan settings are user configured either for speed of data collection or for high data density. For example, a typical scene of 1.2 × 10^6 to 1.8 × 10^6 points can be acquired in 10–15 min. The laser pulse has an approximate footprint of 15 mm diameter at a range of 50 m, with spot spacings as low as 10 mm. These specifications potentially allow the sensor to receive a backscatter signal from deep within dense canopies and sample the complete two-dimensional area of the 40° × 40° field of view at distances up to 100 m away from the sensor.

Plots C and D were surveyed by Optech Inc. with the ILRIS-3D sensor over a 6-h period on 5 July 2002. Since this study tests a new application of ground-based laser scanning technology, an optimal scan configuration has not been established. For this study, it was decided that for each plot all scans would originate outside of the plot boundaries and converge on a clearly identifiable central feature within the plot. Positioning of each ILRIS-3D base station was limited by local site conditions and plot visibility. The locations of the ILRIS-3D base station are presented in Fig. 2. For all scans, the laser head was elevated between 1.4 and 1.8 m above ground level, with the scanner axis tilted slightly upwards at an angle between 10° and 20° above horizontal to ensure maximum scan coverage within the canopy.

Five scans of data were collected for each plot, plus two further scans (12 scans total) along a pathway between the two plots to facilitate accurate spatial coregistration of all lidar data. To ensure that all scans could be aligned (coregistered), approximately 10 small control marker targets that were visible from multiple sensor locations were erected in each of the plots. Five of the control markers were statically DGPS surveyed (referenced to a base station 40 km south of the study area) to facilitate georegistration of the ILRIS-3D point cloud data (a minimum of three are required). Alignment and subsequent georegistration of the raw ILRIS-3D data were carried out by Optech Inc. using the IMAlign module within the Polyworks software suite (InnovMetrics Software Inc., Sainte-Foy, Que.). The scan alignment procedure required coarse visual alignment of the scans prior to computing the best fit using an automated iterative three-dimensional registration algorithm that relies on lidar point cloud residual calculations within the scan overlap region. The merged raw point cloud data (each point represented by a unique easting, northing, and elevation coordinate) were then analysed for forest metric information.

Lidar data analysis

Tree identification

At this early stage in the development of this technical application, automated feature recognition routines to identify and extract trees from the lidar point cloud were unavailable and so manual techniques using objective decision criteria were the only option (see Figs. 3 and 4 for side views of the lidar point cloud data for plots C and D, respectively). To isolate and identify individual tree locations within the lidar point cloud, it was assumed that each tree stem would be represented by a distinct arc or enclosed circle of lidar points (when viewed from above), which would be a distance several factors greater than the stem diameter away from adjacent tree stems. It follows, therefore, that individual tree stems can be visually discriminated and isolated from the surrounding point cloud data associated with the ground, forest debris, and foliage. Exceptions are possible in cases where a tree stem is split, where a small tree and a large tree are in close proximity to one another, or where a stem is completely obstructed from the ILRIS-3D's view by intervening material.

To perform this tree stem identification, it was necessary to temporarily remove the point cloud data associated with the ground, tree canopies, and low understory. This was attempted by extracting a horizontal layer of data that corre-

Fig. 3. Side view of the red pine plantation (plot C) lidar tree point clouds within the Polyworks' IMInspect module.

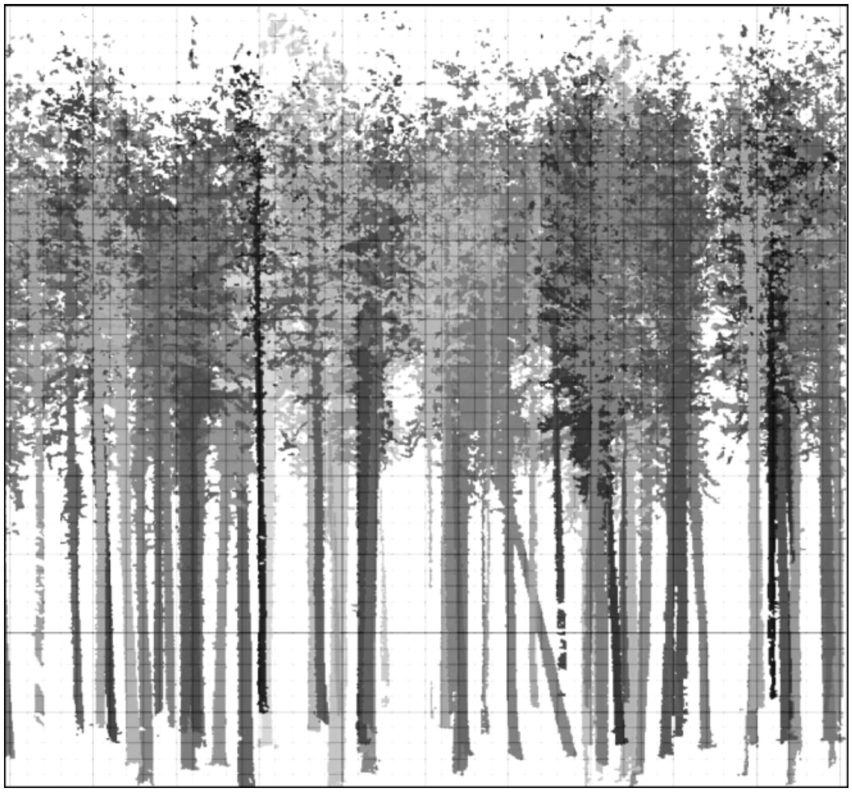

Fig. 4. Side view of the mixed deciduous stand (plot D) lidar tree point clouds. Note reduced data density at top levels of canopy.

sponded predominantly to tree stems only. For plot C the horizontal layer corresponded to heights that were approximately 1 to 4 m above the average ground height. For plot D, a slightly elevated range of approximately 2 to 7 m above average ground height was chosen because of the dense understory and irregular tree positions within the plot.

After slicing the lidar point cloud data to leave behind a tree stem layer, the manually surveyed tree location map was overlaid on the sliced point cloud layer to assess the correspondence between the two data sets (Fig. 5). For the lidar tree stems that were identified as corresponding to manually surveyed trees, the tree stem centre coordinate was computed within the Polyworks software environment as the centre of the arc or circle of lidar points defining the tree stem. For the few tree stems not obviously identifiable from the sliced point cloud, a visual inspection of the entire point

Fig. 5. Manually surveyed tree locations (crosses) overlaid on sliced point cloud layers for subareas within plot C (left) and plot D (right) prior to positional adjustments. Line vectors illustrate the offset between POS LS and ILRIS-3D tree stem locations. Note the presence of low tree canopies in plot D.

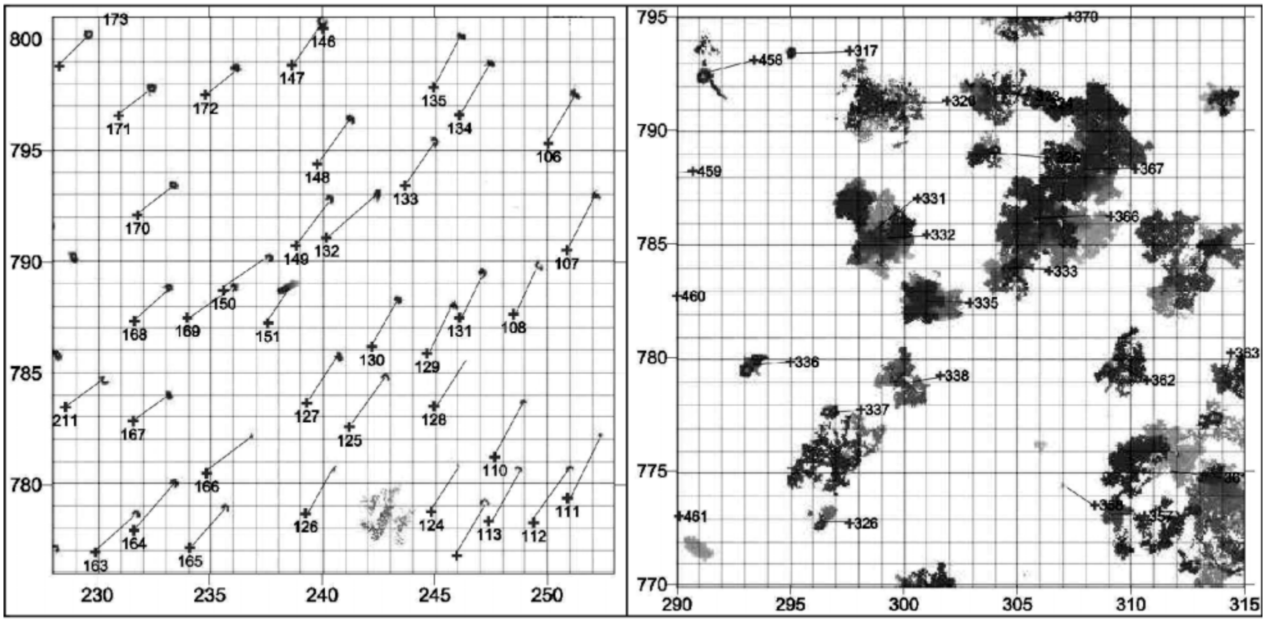

cloud was carried out in the vicinity of the manually surveyed location. All trees could be easily identified by this second technique, but it was not a preferred method because of the level of subjective interpretation and its reliance on previously surveyed ground data. The lidar-based location of these trees was defined as the centre coordinate of a vector joining the lowest and highest points within the respective tree's point cloud. Plot D required more manual interpretation of lidar tree locations because of the wide range of tree heights and overlapping canopies within the plot. All the lidar-derived locations could then be directly compared with the field validation data to ascertain tree identity and estimate overall positional discrepancies between the two methods (Fig. 5).

It is important to note here that comparing the tree location maps using the technique described was carried out to facilitate tree-level comparisons of manually measured and lidar-derived metric information. This was not carried out to test the utility of the ILRIS-3D sensor for tree stem mapping. Although it should further be noted that with refinements of the techniques used here and feature recognition algorithms, automated stem mapping and tree extraction from the ILRIS-3D point cloud data are conceivable and should be evaluated more thoroughly.

Extracting trees from the lidar point cloud

The lidar point clouds associated with individual trees were separated from one another and were numbered in accordance with the tree tag identifiers placed on each tree in the field. This task was carried out in the Polyworks software environment, using the IMInspect module. The selection of all point cloud data associated with a single tree was performed by locating each tree stem coordinate within the entire plot point cloud and then setting a horizontal radius corresponding to maximum crown diameter around this point. In most cases this generated point clouds for each tree that extended beyond the actual limits of the tree crown and often included portions of canopy from neighbouring trees and, in the case of plot D, understory and overstory. All individual tree point clouds were visually inspected, and outlying point cloud data that were obviously not associated with the tree in question (i.e., lidar returns from surrounding vegetation) were manually deleted. This was a manually intensive task, but given the high sample point density throughout the plots and the multiple view locations of the ILRIS-3D sensor, discriminating between points associated with a particular tree and the surrounding foliage was generally straightforward.

Tree height

Each individual tree point cloud was imported into IMInspect so that tree metrics could be extracted from the point cloud. Tree height was estimated by fitting a vector primitive to the data corresponding to the visible height of the tree (Fig. 6). This procedure was objective, as the tree height was defined by the vector joining the lowest and highest elevation points within an individual tree point cloud. Lidar-derived height estimates for each tree were then compared with field-validation measurements.

Stem DBH

Tree stem diameter for individual tree point clouds was estimated by selecting all lidar point data that lay between 1.25 and 1.75 m vertically above the lowest point in the file, and then fitting a cylinder primitive to the data (Fig. 7). The method used in the software to perform the best fit to the lidar tree stem data was a cylindrical least squares regression performed on the surface arc or cylinder defined by the lidar points that were reflected from the stem. The number of stem lidar points used for the DBH regression calculations ranged from 100 to greater than 2000 points. Trees with no points in the section of stem selected or displaying insuffi-

Fig. 6. Tree height estimated as length of line (vector primitive) joining highest to lowest points within each tree's lidar point cloud.

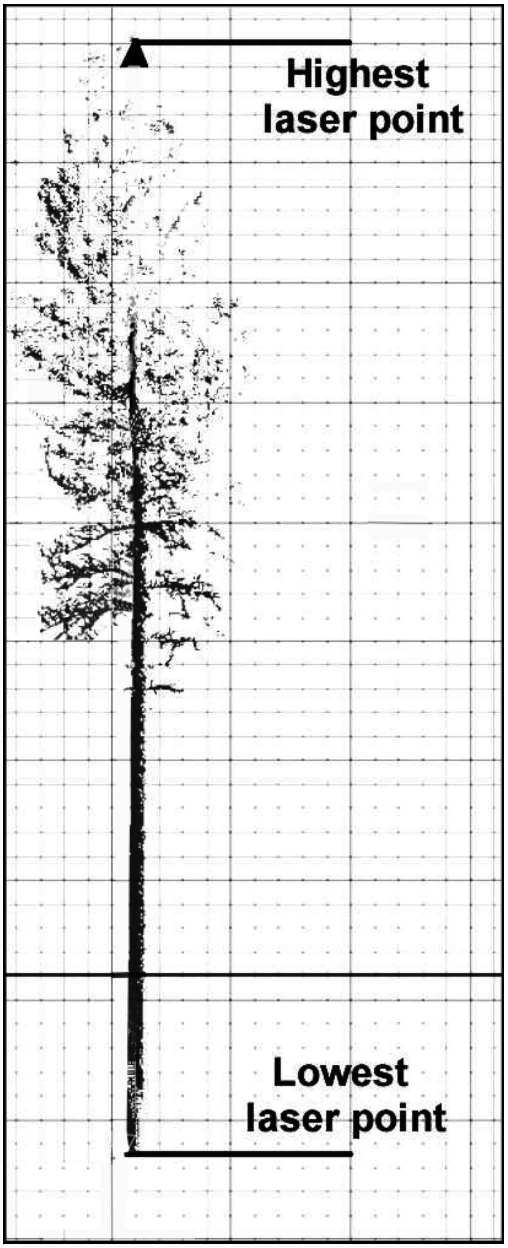

cient data to adequately define the arc around the stem were omitted from the analysis.

Forest mensuration statistics

From both the field-validation measures and equivalent lidar-derived height and DBH data, summary statistics of derived forest metric parameters were calculated to facilitate comparisons. The statistics generated for each plot included (*i*) stem density (no./ha), (*ii*) total basal area (m^2/ha), (*iii*) gross total tree volume (m^3), and (*iv*) merchantable volume (m^3).

Gross total and merchantable volume estimates for both plots were calculated using allometric equations used by the local forest manager (C. Gynan, Silv-Econ Ltd., personal communication), which were developed by Bonnor and Magnussen (1986). Volume estimates were calculated from both the field-validation measures and lidar-derived height, DBH, and stem density measurements. Plot-level estimates were made using data collected from trees with a DBH of 10 cm or greater. For details of the allometric equations used the reader is referred to Bonnor and Magnussen (1986).

Results and discussion

Scan coverage summary

From all 12 scans, more than 14.5×10^6 lidar points were recorded, with approximately 4×10^6 of these falling within each plot. For an approximate plot volume of 35 m × 35 m × 25 m, this gives a mean sampling point density of 130 points/m^3, but considering that most of the volume in the plots is empty space, the actual sampling density within volumes occupied by vegetation was several factors higher than this and highly variable.

Both plots have the same area, but the complete horizontal scan coverage for the overlapping field of view from the five ILRIS-3D base locations in each plot varies. For areas covered by at least a single scan, plot D displays almost complete coverage at over 97% (69% in areas of three intersecting scans), and plot C displays almost complete coverage at around 95% (51% with three intersecting scans). The greater single- and multiple-scan coverage for plot D can be attributed to a slightly more uniform distribution of ILRIS-3D base locations around the plot (Fig. 2). Subsequent stem density and volume calculations are corrected for the total area of single scan coverage, for example, ILRIS-3D derived plot stem density (no./ha) is calculated from the number of trees observed within the total plot area that contains at least one scan coverage.

Tree locations and stem density

The number of trees above 2 m in height measured manually in the field was 81 and 57 (138 total) for plots C and D, respectively, compared with 77 and 57 (134 total) extracted from the ILRIS-3D point cloud data. The horizontal planimetric errors based on a comparison of the manual tree surveys and the 134 lidar-derived tree locations are presented in Table 1. The proportion of the total number of trees within each plot that were extracted from the lidar data approximately corresponded to the total aerial scan coverage proportion, i.e., for plot C the 77 trees extracted from the lidar data equaled 95% of the 81 trees within the plot, and this proportion also equaled the plot area that was covered by at least a single scan. Therefore, the stem density estimate of 661 stems/ha for plot C was identical using both techniques. For plot D, all 57 trees were identified within the ILRIS data despite a scan coverage of >97%. This led to a slightly higher estimate of stem density using the lidar-derived data (480 stems/ha lidar compared with 465 stems/ha manual).

Within both plots, there was an offset between lidar and manual tree location measurements. Some systematic bias is likely attributable to the different survey monuments and methods used to register the lidar control points (DGPS) and the manual tree surveys (POS LS and triangulation). In addition, the alignment and georegistration processes could introduce slight warp into the merged scan data as a result of

Fig. 7. Tree stem DBH estimation using simple cylindrical primitive fitted to the tree stem lidar point cloud between 1.25 and 1.75 m above the ground level (0.00 m is assumed to correspond to the lowest lidar point within an individual tree's point cloud).

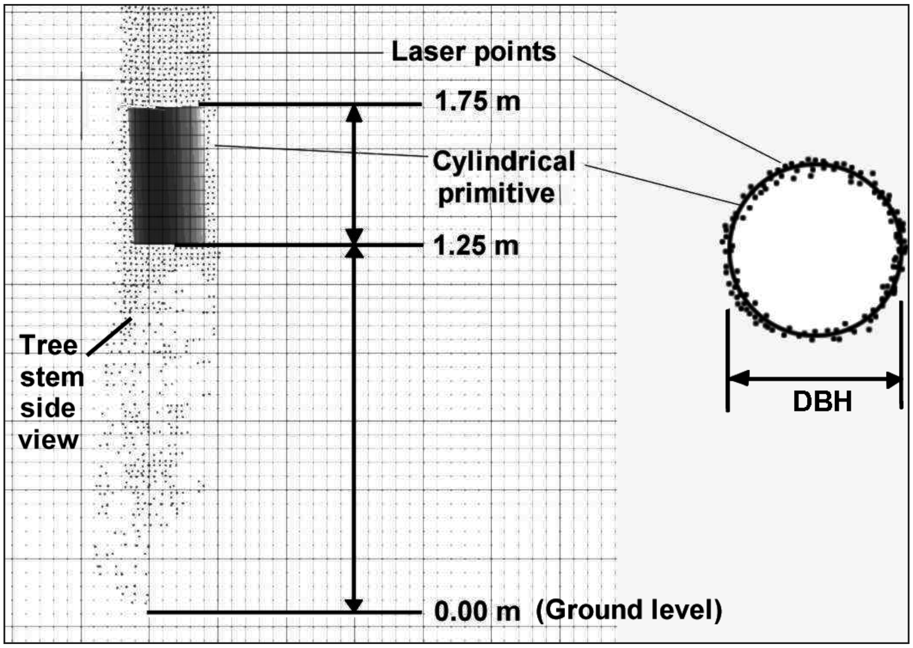

Table 1. Offset between lidar-derived and manually surveyed tree locations for both plots.

	Manual – lidar coordinate offset (m)	
Statistics	Easting	Northing
Plot C		
Mean	–1.5	–1.7
Minimum	–2.3	–2.6
Maximum	0.3	–0.7
Standard deviation	0.3	0.5
No. of trees (arc, vector)*	77 (70, 7)	
Manual survey technique	56 POS LS, 21 triangulation	
Plot D		
Mean	2.4	–0.7
Minimum	1.1	–2.7
Maximum	5.0	0.5
Standard deviation	0.9	0.8
No. of trees (arc, vector)*	57 (51, 6)	
Manual survey technique	1 POS LS (centre tree), 56 triangulation	

*The total number of measurements is also broken down into number of trees derived by a stem arc centroid coordinate from the sliced point cloud or from a vector centroid coordinate (see text).

imperfect alignment and control point inaccuracies; both of these problems pose significant challenges within forested environments. Lidar and manual tree locations tended to be closer in plot C than in plot D, and this is likely attributable to increased manual survey errors in the deciduous plot owing to triangulation from a single known point. However, all lidar-derived trees were within 5 m of their ground-surveyed location, with a mean offset of around 2 m. It cannot be stated with certainty that there have been no errors of commission or omission, but the correspondence of the tree counts, the generally small locational errors, and the ease with which individual trees could be identified within the lidar point cloud suggest that all trees were correctly identified within those areas of the plots covered by a single scan.

Although locating and counting trees with lidar point cloud data has been shown to be achievable here, prior knowledge of tree numbers and locations was already available for this study, and combining the two data sets aided in the interpretation of the lidar data. This is important because isolating individual tree stems using the simple vertical slicing procedure was more difficult in plot D because of the multitiered and overlapping nature of the deciduous canopies (Figs. 4 and 5). Fortunately, this was not a problem in plot C (Figs. 3 and 5), as all tree stems could be easily discriminated. Therefore, lidar point cloud data do offer the potential for automated tree identification, counting, and location estimation, but in forest areas other than uniform single-tier plantations, this process would require substantial manual interpretation, or some kind of sophisticated feature recognition and extraction process.

Tree height and DBH

Summary tree height and DBH statistics for the manual and lidar measurement methods are presented in Table 2 and illustrated in Figs. 8 and 9. Results indicate that there is reasonable correspondence between manual and lidar estimates of tree height and DBH. For DBH, there was no systematic tendency for lidar to under- or over-estimate the field validation measures. For tree height, however, there was a tendency for the ground-based lidar to underestimate the field validation value by approximately 1.5 m (~7% of mean height) for trees within both plots. This was generally a function of low sample point density in the upper canopy (see Figs. 3, 4, and 6), which can be attributed to (*i*) the influence of shadowing caused by the lower canopy, and (*ii*) suboptimal sampling with the ILRIS-3D. As was stated earlier, the positioning of ILRIS-3D survey stations around the plots was not uniform (see Fig. 2), with some stations too close to the plot to completely sample the vertical canopy profile. Therefore, although the aerial extent of each plot was well represented in the aligned scans, the upper part of the vertical profile within each plot was not. This is due to the ILRIS-3D field of view limitation of 40° and is a critical element of sampling design that requires further attention for future studies. For example, smaller plots, data collection during leaf-off conditions, more numerous and distant scan locations, and increased vertical scan angle are measures that would improve lidar sampling of the upper canopy.

Some height measurement error (lidar and manual) occurs as a result of intervening foliage obstructing the view to the top or bottom of trees. This potentially leads to systematic lidar height underestimations (particularly for the tallest trees) because of canopy shadowing. This is illustrated in Fig. 8, where it is apparent that (*i*) the agreement between manual and lidar height estimates is weakest for the tallest trees, and (*ii*) the best-fit line has a gradient greater than unity because of the tendency for lidar to underestimate tree height in the upper canopy. Figure 8 also illustrates that residual dispersion along the regression line is slightly greater for the deciduous plot. This observation concurs the findings of Williams et al. (1994) that tree height measurements tend to be less accurate in hardwood stands than softwood stands.

The combined regression plot gradient of 1.08 with an r^2 of 0.85 illustrates that ground-based lidar is potentially a useful technique for estimating the heights of trees, but when viewing the regression plots for each site type independently, it is apparent that this relationship is site dependant. The slope and r^2 for plot D (1.09 and 0.86, respectively) are close to the combined regression statistics, but for plot C the regression slope and r^2 (0.31 and 0.13, respectively) do not indicate a good relationship. However, given the homogeneity of tree dimensions in the red pine plantation, tree heights are clustered around the mean height of 23.6 m. As such, regression is not an appropriate method of evaluation, and the summary statistics in Table 2 should be considered a more appropriate means of assessing the capability of the laser scanner technology for height estimation in a conifer plantation. With improved vertical scan distribution throughout the sample plots, it is likely that lidar height estimates would improve.

Table 2. Plot-level statistics of tree height and DBH estimates using lidar and manual measurement techniques.

	Height (m)		DBH (m)	
Statistics	Lidar	Manual	Lidar	Manual
Plot C				
Mean	22.1	23.6	0.26	0.27
Minimum	19.3	19.6	0.08	0.20
Maximum	24.3	26.1	0.39	0.37
Standard deviation	1.2	1.0	0.06	0.03
No. of trees	76	81	70	81
Plot D				
Mean	17.9	19.4	0.25	0.24
Minimum	2.8	2.7	0.04	0.02
Maximum	24.3	30.8	0.57	0.62
Standard deviation	6.4	7.8	0.13	0.14
No. of trees	56	57	51	57

DBH shows a good linear relationship (r^2 = 0.85) that is very close to unity between lidar and manual validation measurements (Fig. 9). When both plots are considered separately, it is apparent that the strength of the relationship differs, with r^2 values of 0.54 and 0.98 for plot C and D, respectively. The poor r^2 value for plot C is, again, a function of the homogeneity of tree dimensions within the pine plantation. Of note is that the residual dispersion for plot C in Fig. 9 is greater than that for plot D, despite both the range and absolute DBH values being higher in plot D. The greater magnitude of residual dispersion suggests that it was more difficult to accurately estimate DBH from the lidar data in the homogeneous conifer plantation than in the highly heterogeneous and multitiered mixed deciduous stand.

The automated alignment of individual scans posed a challenge in forest environments because of the need for well-defined unique features in the lidar point cloud data to enable an accurate least squares three-dimensional registration in the overlap region of multiple scans. This was particularly apparent in the conifer plantation, as the trees possessed similar characteristics and there were few easily identifiable control points. After closer inspection of the sliced point cloud data (an overview is provided in Fig. 5), it was apparent that some of the tree stems around the edge of plot C were composed of multiple scans that did not align perfectly. In some cases, the scans of the stem did not merge uniformly around the stem but rather intersected, leading to an apparently smaller stem, or in other cases the scans did not quite meet, thus resulting in a slightly large lidar definition of the stem. This effect could be minimized in future forest ground-based lidar data collections by placing more numerous and distinctive control markers throughout the plot than were used for this study.

Volume estimation

Summaries of the plot-level volume calculation statistics

Fig. 8. Regression plots of manual versus lidar tree height estimates for both plots. Residual plot shown in inset.

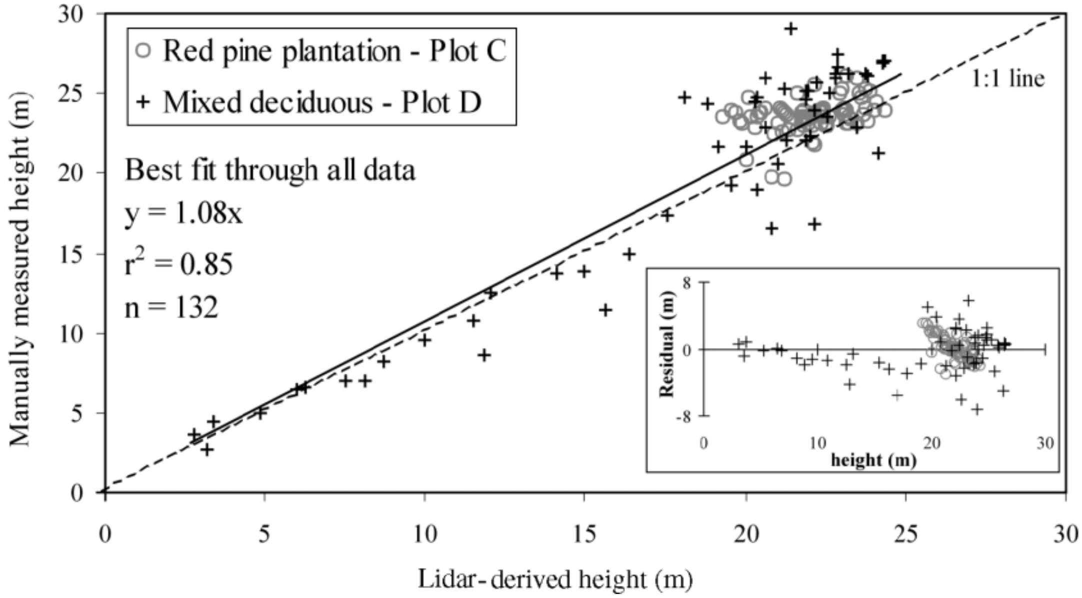

Fig. 9. Regression plots of manual versus lidar DBH estimates for both plots. Residual plot shown in inset.

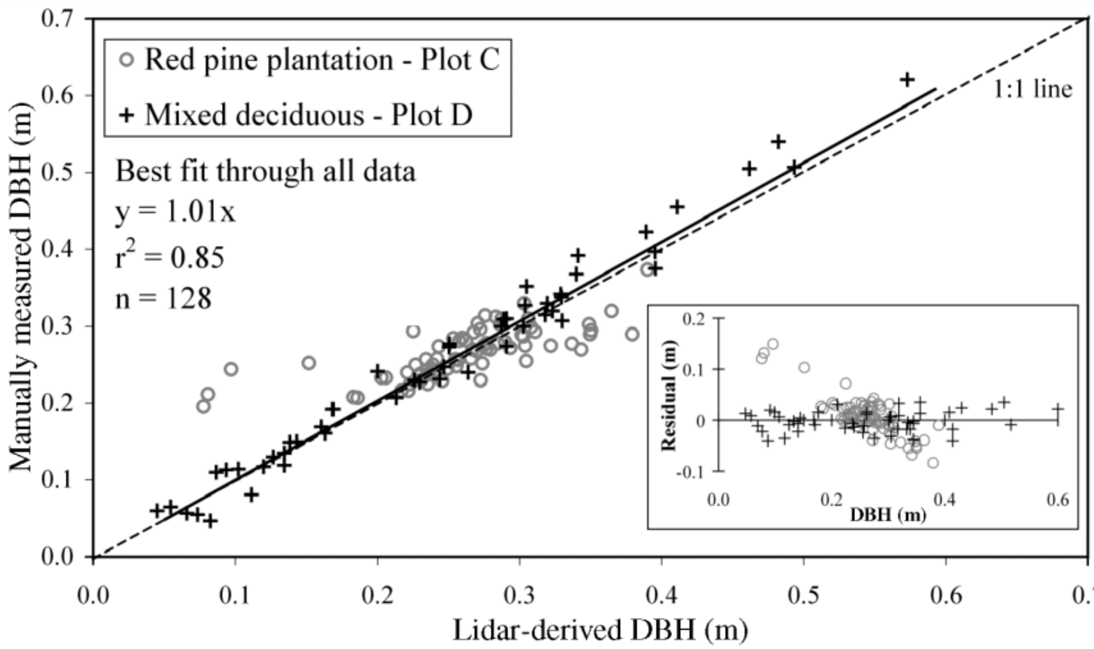

generated from allometric equations using the height, DBH, and area estimates above are presented in Table 3. Both lidar-derived estimates of volume are within 7% of those calculated from manual field measurements. For the conifer plantation (plot C), the lidar data provide a slight underestimation of both gross and merchantable volume, and this is attributable to slight underestimations of both DBH and tree height. However, for the deciduous stand (plot D), the lidar data slightly overestimate gross and merchantable volume because of a slight overestimation of stem density.

Table 3. Summary of volume calculation statistics derived from manual and lidar measurement techniques for both plots.

	Plot C		Plot D	
Volume calculation statistics	Manual	Lidar	Manual	Lidar
Stem density (no./ha)	661	661	465	480
Total basal area (m^2/ha)	37.4	37.2	28.5	28.3
Gross total tree volume (m^3)	107.5	100.8	53.3	56.3
Merchantable volume (m^3)	103.7	97.1	48.0	50.7

Conclusions

Ground-based scanning lidar technology has been shown to be useful for forest metric assessment, with the potential to provide objective measures of tree location, tree height, DBH, stem density, and plot-level volume that are comparable with more traditional techniques. In the sample data collected there was a tendency for the lidar data to underestimate the mean plot-level tree height values by approximately 1.5 m compared with manual measurements. This result was attributed to canopy shadow effects and incomplete sampling of the vertical plot profile. DBH measurements extracted from the ILRIS-3D data agreed well with manual measurements, despite difficulties aligning the individual lidar scans in the homogeneous red pine plantation. Lidar derived gross and merchantable timber volumes for both stands were within 7% of estimates derived from manual measurements.

Manual field mensuration of all trees within a plot can be time consuming, and measurements are susceptible to subjective interpretation. The potential speed and objectivity of data collection and extraction available with the ground-based scanning lidar techniques are desirable attributes. With the development of automated forest mensuration data extraction routines, tree-level measurements would be objective (i.e., arrived at in a consistent and repeatable manner), and the time to process the data through to plot-level statistics and volume estimates could potentially be faster than traditional techniques. However, because of analytical constraints in currently available software, the work presented here was manually intensive, required a helping hand from the manual survey data, and substantial work is needed to develop automated data extraction and assessment methods.

In this paper, simple forest inventory parameters have been extracted from the lidar point cloud data. However, it should be apparent that with the capability to laser scan an entire plot, it is possible to remotely sample the entire plot volume and thus create a three-dimensional digital model of the canopy and understory structure without disturbing the plot. These data therefore also could be used for analyses of forest stand structure, vertical and horizontal foliage distribution, canopy light transfer, leaf or foliage area indices, and high-resolution virtual faunal habitat reconstruction. Future tests and development of the technology for forestry applications should perhaps concentrate on smaller permanent growth and yield plots, where detailed and frequently monitored forest metric data, including stem maps, are available, and where the lidar application emphasis would be on change monitoring rather than inventory.

Acknowledgements

We thank Optech Incorporated for providing and operating the ILRIS-3D laser imager and a 2-week software license of the Innovmetric Polyworks suite; Applanix for providing and operating their prototype POS LS inertial surveying equipment to survey in some of the tree stem locations; Mr. Chris Gynan of Silv-Econ Ltd. for assisting with plot selection; The Canadian Consortium for LiDAR Environmental Applications Research (C-CLEAR) for supporting this project.

References

Aldred, A.H., and Bonner, G.M. 1985. Application of airborne laser to forest surveys. Can. For. Serv. Petawawa Natl. For. Inst. Inf. Rep. PI-X-51.

Applanix Inc. 2001. POS LS technical note. Applanix Inc., Toronto, Ont.

Bachman, C.G. 1979. Laser radar systems and techniques. Artech House, Norwood, Ma.

Baltsavias, E.P. 1999. Airborne laser scanning: basic relations and formulas. ISPRS J. Photogramm. Remote Sens. **54**: 199–214.

Bonnor, G.M., and Magnussen, S. 1986 Inventory and growth predictions of the Petawawa Research Forest. Can. For. Serv. Petawawa Natl. For. Inst. Inf. Rep. PI-X-66.

Bruce, D. 1975. Evaluating accuracy of tree measurements made with optical instruments. For. Sci. **21**: 421–426.

Hopkinson, C., Sitar, M., Chasmer, L.E., and Treitz, P. 2004. Mapping snowpack depth beneath forest canopies using airborne LiDAR. Photogramm. Eng. Remote Sens. **70**(3): 323–330.

Lichti, D.D., Stewart, M.P., Tsakiri, M., and Snow, A.J. 2000. Benchmark tests on a three-dimensional laser scanning system. Geomat. Res. Aust. **72**: 1–23.

Lichti, D.D., Gordon, S.J., and Stewart, M.P. 2002. Ground-based laser scanners: operation, systems and applications. Geomatica, **56**: 21–33.

Lim, K., Treitz, P., Baldwin, K., Morrison, I., and Green., J. 2003*a* Lidar remote sensing of biophysical properties of northern tolerant hardwood forests. Can. J. Remote Sens. **29**: 658–678.

Lim, K., Treitz, P., Wulder, M., St-Onge, B., and Flood, M. 2003*b*. LiDAR remote sensing of forest structure. Prog. Phys. Geogr. **27**(1): 88–106.

Lovell, J.L., Jupp, D.L.B., Culvenor, D., and Coops, N.C. 2003. Using airborne and ground based ranging Lidar to measure canopy structure in Australian forests. Can. J. Remote Sens. **29**: 607–622.

Maclean, G.A., and Martin, G.L. 1984. Merchantable timber volume estimations using cross-sectional photogrammetric and densitometric methods. Can. J. For. Res. **14**: 803–810.

Magnussen, S., and Boudewyn, P. 1998. Derivations of stand heights from airborne laser scanner data with canopy-based quantile estimators. Can. J. For. Res. **28**: 1016–1031.

Manninen, A.T., Rautakorpi, K.S., and Rantasuo, M.S. 1999. Effects of tree structure on backscattering *In* Proceedings of the International Geoscience and Remote Sensing Symposium, 28 June – 2 July 1999, Hamburg, Germany. The International Geoscience and Remote Sensing Society [CD-ROM].

Næsset, E. 1997*a*. Determination of mean tree height of forest stands using airborne laser scanner data. ISPRS J. Photogramm. Remote Sens. **52**: 49–56.

Næsset, E. 1997*b*. Estimating timber volume of forest stands using airborne laser scanner data. Remote Sens. Environ. **61**: 246–253.

Nelson, R., Krabill, W., and Maclean, G. 1984. Determining forest canopy characteristics using airborne laser data. Remote Sens. Environ. **15**: 201–212.

Radtke, P.J., and Bolstad, P.V. 2001. Laser point-quadrat sampling for estimating foliage-height profiles in broad-leaved forests. Can. J. For. Res. **31**: 410–418.

Schumacher, F.X., and Hall, F. 1933. Logarithmic expression of timber-tree volume. J. Agric. Res. **47**: 719–734.

Tanaka, T., Yamaguchi, J., and Takeda, Y. 1998, Measurement of forest canopy structure with a laser plane range-finding method — development of a measurement system and applications to real forests. Agric. For. Meteorol. **91**: 149–160.

Welles, J.M., and Cohen, S. 1996. Canopy structure measurement by gap fraction analysis using commercial instrumentation. J. Exp. Bot. **47**: 1335–1342.

Williams, M.S., Bechtold, W.A., and La Bau, Y.J. 1994. Five instruments for measuring tree-height: an evaluation. South. J. Appl. For. **18**: 76–82.